Ann. Geophys., 26, 1919–1933, 2008
www.ann-geophys.net/26/1919/2008/

Annales Geophysicae

Estimates of magnetic cloud expansion at 1 AU

R. P. Lepping[1], C.-C. Wu[1,2], D. B. Berdichevsky[1,3], and T. Ferguson[4]

[1]Space Weather Laboratory, NASA-Goddard Space Flight Center, Greenbelt, MD 20771, USA
[2]University of Alabama in Huntsville, AL 35899, USA
[3]Sigma Space Corporation, 4801 Forbes Boulevard, Lanham, MD 20706, USA
[4]University of Richmond, 28 Westhampton Way, University of Richmond, VA 23173, USA

Received: 11 March 2008 – Accepted: 26 May 2008 – Published: 16 July 2008

Abstract. In this study we analyze 53 magnetic clouds (MCs) of standard profiles observed in WIND magnetic field and plasma data, in order to estimate the speed of MC expansion (V_E) at 1 AU, where the expansion is investigated only for the component perpendicular to the MCs' axes. A high percentage, 83%, of the good and acceptable quality cases of MCs (N(good)=64) were actually expanding, where "good quality" as used here refers to those MCs that had relatively well determined axial attitudes. Two different estimation methods are employed. The "scalar" method (where the estimation is denoted $V_{E,S}$) depends on the average speed of the MC from Sun-to-Earth ($<V_{\mathrm{S-to-E}}>$), the local MC's radius (R_O), the duration of spacecraft passage through the MC (at average local speed $<V_C>$), and the assumption that $<V_{\mathrm{S-to-E}}>=<V_C>$. The second method, the "vector determination" (denoted $V_{E,V}$), depends on the decreasing value of the absolute value of the Z-component (in MC coordinates) of plasma velocity ($|V_Z|$) across the MC, the closest approach distance (Y_O), and estimated R_O; the Z-component is related to spacecraft motion through the MC. Another estimate considered here, $V'_{E,V}$, is similar to $V_{E,V}$ in its formulation but depends on the decreasing $|V_Z|$ across part of the MC, that part between the maximum and minimum points of $|V_Z|$ which are usually close to (but not the same as) the boundaries points. The scalar means of estimating V_E is almost independent of any MC parameter fitting model results, but the vector means slightly depends on quantities that are model dependent (e.g. $|CA|\equiv|Y_O|/R_O$). The most probable values of V_E from all three means, based on the full set of N=53 cases, are shown to be around 30 km/s, but V_E has larger average values of $<V_{E,S}>$=49 km/s, $<V_{E,V}>$=36 km/s, and $<V'_{E,V}>$=44 km/s, with standard deviations of 27 km/s, 38 km/s, and 38 km/s, respectively. The linear correlation coefficient for $V_{E,S}$ vs. $V'_{E,V}$ is 0.85 but is lower (0.76) for $V_{E,S}$ vs. $V_{E,V}$, as expected. The individual values of V_E from all three means are usually well below the local Alfvén velocities, which are on average (for the cases considered here) equal to 116 km/s around the inbound boundary, 137 km/s at closest approach, and 94 km/s around the outbound boundary. Hence, a shock upstream of a MC is not expected to be due to MC expansion. Estimates reveal that the errors on the "vector" method of estimating V_E (typically about $\pm$7 km/s, but can get as large as $\pm$25 km/s) are expected to be markedly smaller than those for the scalar method (which is usually in the range $\pm(15\Leftrightarrow20)$ km/s, depending on MC speed). This is true, despite the fact that $|CA|$ (on which the vector method depends) is not always well determined by our MC parameter fitting model (Lepping et al., 1990), but the vector method only weakly depends on knowledge of $|CA|$.

Keywords. Interplanetary physics (Interplanetary magnetic fields; Solar wind plasma) – Solar physics, astrophysics, and astronomy (Flares and mass ejections)

1 Introduction

In the past, observations of the speed profile of the solar wind within an interplanetary magnetic cloud (MC) at 1 AU were used in determining whether the cloud was expanding or not locally (e.g. Burlaga, 1990; Farrugia et al., 1992a, b, 1993). For MC expansion the speed must show a marked, and approximately linear, decrease across the cloud or across most of it; see Fig. 1. Earlier studies have, in fact, shown that it was not uncommon for MCs at 1 AU to be expanding (e.g. Burlaga, 1995; Hidalgo, 2003, 2005), and it was determined from WIND data that a large percentage of MCs seen at 1 AU are expanding (Lepping et al., 2002). Briefly, a MC was defined empirically by L. Burlaga and coworkers as a (usually large) interplanetary structure having enhanced field

Correspondence to: R. P. Lepping
(ronald.p.lepping@nasa.gov)

Published by Copernicus Publications on behalf of the European Geosciences Union.

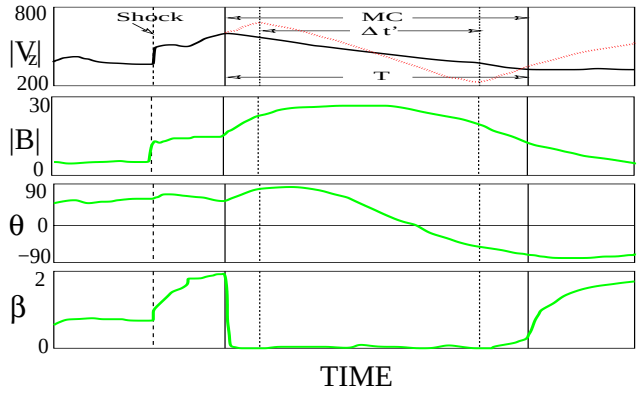

Fig. 1. A cartoon stressing the profile of the observed $|V_Z|$ ($\equiv|V_{Z,CL}|$) gradient of velocity as the spacecraft passes through a MC that is expanding; the subscript CL refers to the MC coordinate system (see Sect. 2), where the $\mathbf{X}_{CL}$-axis is aligned with the estimated local axis of the MC. Also shown (in green) are the magnetic field magnitude, field latitude angle, and proton plasma beta. The duration of the MC passage is T and the interval from the MAX to MIN of $|V_{Z,CL}|$ is $\Delta t'$. A upstream shock ramp is indicated for this MC, even though not all MCs possess upstream shocks. The red dashed curve for $|V_{Z,CL}|$ holds for a case where the MAX and/or MIN points for this quantity are markedly different from its values at the boundaries, and the black curve for $|V_{Z,CL}|$ holds for the case when its MAX and MIN values are at or very near to the boundaries.

magnitude, a relatively smooth change in field direction as the observing spacecraft passes through the MC, and lower proton temperature (and proton beta) than the surrounding solar wind. MC properties were first discussed by Burlaga et al. (1981), Goldstein (1983), and Burlaga (1988, 1995). Many believe that eruptive prominences are the main source of MCs (e.g. Bothmer and Schwenn, 1994). Also it is believed that MCs are essentially the "core" of Interplanetary Coronal Mass Ejections (ICMEs); e.g. see Gopalswamy et al. (1998), and also see early reviews by Gosling (1990, 1997) that compare CMEs to large magnetic flux ropes in the solar wind which are usually the essence of MCs.

The main purpose of this study is to analyze quantitatively MC expansion using WIND magnetic field and solar wind velocity data. The ultimate goal of the study is to use our resulting understanding of MC expansion to modify, as accurately as possible, a static MC parameter fitting program (Lepping et al., 1990) to accommodate 3-D expanding MCs, as well as to accommodate other features (e.g. non-circular cross-section), in a systematic production mode; the original fitting program (using only a static model) was also capable of working in a production mode. For this study 100 WIND MCs, covering the 11-year period from early 1995 to about August 2006 have been identified and parameter-modeled, and after "editing" in two stages was reduced to N=53 cases. The two stages consist of, first, quality editing, described in detail below, and then a test for appropriateness (i.e. we ask: Was the MC actually expanding or not?). For the MC fitting itself (Lepping et al., 1990) only an average MC speed was required, in order to transform from the time domain to the space domain. Then the resulting estimated radius, called R_O, from the static flux rope modeling is assumed useful for carrying over to the actually expanding cases by viewing R_O as a weighted average of a continuum of radii during cloud passage. The view was (and is) that at first encounter the flux rope's radius was at a minimum and expanding to a maximum upon departure. It is also assumed that any non-circular cross-section effects are less important, even though it is very likely that cases of perfectly circular cross-sections at 1 AU are probably rare; see, e.g. Riley and Crooker (2004). There have been many hypotheses concerning the true nature of this radial expansion of MCs and how it is detected (e.g. Marubashi, 1986, 1997; Farrugia et al., 1992a, b; Burlaga, 1995; Osherovich et al., 1993, 1995; Mulligan and Russell, 2001; Berdichevsky et al., 2003). In such studies usually only one or two examples of MCs are examined in determining the nature of the velocity profile, but the results may not be characteristic of interplanetary MCs in general. Modern models of MC parameter fitting usually take into consideration MC expansion, as well as other important features, such as the good probability of a MC having a non-circular cross-section; see, for example, Hidalgo et al. (2002), Riley et al. (2004), and Nieves-Chinchilla et al. (2005).

In this study we aim: (1) to estimate quantitatively the rate of expansion of a large number of MCs at 1 AU using two different methods and compare the results of the two methods, and (2) to ascertain the importance of expansion in MC parameter fitting models, for the practical purpose of modifying such a model, which assumes a MC is a simple static force free structure with a circular cross-section. And we examine a large number of cases. We deal here only with MC expansion that is perpendicular to the MC axis. It has been determined that MC expansion in actuality is also along the MC's axis as well, as it must be for full 3-D expansion, but this is much more difficult to determine empirically and accurately; see Berdichevsky et al. (2003), who describe such expansion and give examples of it. We argue that if the expansion is approximately isotropic in 3-D at 1 AU, then by determining the 2-D expansion, i.e. the expansion perpendicular to the MC axis, we are obtaining important information on the axial expansion as well.

2 Coordinate system utilized

It is necessary to carry out this analysis in what we refer to as **Cl**oud (CL) coordinates, where the $\mathbf{X}_{CL}$-axis is aligned with the estimated local axis of the MC and positive in the direction of the magnetic field along that axis, $\mathbf{Z}_{CL}$ is the positive projection of the trajectory of the passing spacecraft on the cross-section of the MC, and $\mathbf{Y}_{CL}$=$\mathbf{Z}_{CL}\times\mathbf{X}_{CL}$. [Note that since the MC moves directly outward from the Sun, the

relative path of the spacecraft through the MC is positive inward toward the Sun, and therefore, is parallel to the $\mathbf{X}_{\rm GSE}$-axis. For example, for the special case of a MC whose axis is parallel to either $(+)\mathbf{Y}_{\rm GSE}$ or $(-)\mathbf{Y}_{\rm GSE}$, we see that the $+\mathbf{Z}_{\rm CL}$ axis is exactly parallel to the $+\mathbf{X}_{\rm GSE}$ axis, i.e. positive toward to the Sun. Then within the MC the plasma velocity exactly along the $-\mathbf{X}_{\rm GSE}$ axis, for this case, is along $-\mathbf{Z}_{\rm CL}$ and should be expressed as $-\mathbf{V}_{\mathbf{Z},\rm CL}$.] The following Website shows how to develop the specific orthonormal matrix needed to transform any data from geocentric solar ecliptic (GSE) coordinates to CL coordinates for any particular MC: http://lepmfi.gsfc.nasa.gov/mfi/ecliptic.html. Such a matrix, as expected, depends on knowledge of the latitude (θ_A) and longitude (ϕ_A) of that MC's axis and on the polarity of the $+\mathbf{Z}_{\rm CL}$ axis with respect to the GSE system, as described above.

3 The formulation

We will develop two means of estimating a MC's expansion velocity, one (called the **s**calar means) which depends on the size (i.e. radius, R_O, in this case), the duration (T) of the MC passage, and the average local MC speed; we call this **e**xpansion velocity, $V_{E,S}$. The other technique (called the **v**ector means) depends on the gradient of the speed across the MC (strictly on the gradient of $V_{Z,\rm CL}$ across most of the MC (more on that below) and on the relative closest approach distance $|Y_O|/R_O$ ($\equiv$|CA|); we denote this expansion velocity as $V_{E,V}$. Finally, we compare the values of $V_{E,S}$ and $V_{E,V}$ (and a modified form, called $V'_{E,V}$, explained below, will be considered) for our set of 53 MCs. Below we give the specifics of these two techniques.

Some of our results will obviously depend on the technique employed (vector or scalar) and on the MC parameter fitting model, because that is how we obtain needed quantities: MC axis direction (especially for the coordinate transformation), $Z_{\rm CL}$-direction, Y_O, and R_O; these are especially needed for the vector technique. For the scalar technique only R_O is need from the MC fitting model, which is usually well determined (if there is not a gross deviation from a circular cross-section), so this technique is only weakly dependent on the model.

Since modern techniques of estimating MC fitting parameters and global models of MC tend to agree that most MCs do not have circular cross-sections, we do not demand that such be the case either; see e.g. Lepping et al. (1998), Vandas et al. (2002, 2006), Vandas and Romashets (2003), Riley et al. (2004), and Nieves-Chinchilla (2005). However, we assume that the semi-minor axis ($R_{\rm MIN}$) and semi-major axis ($R_{\rm MAX}$) of the MC's cross-section are not vastly different from each other. (We will think of the cross-section as oval, but not necessarily an ellipse, centered at the MC's axis.) That is, we assume that $R_{\rm MAX}/R_{\rm MIN} \lesssim 2$, or so. Then we think of R_O, as estimated by the model of Lepping et al. (1990) as being the average of these two axes lengths, i.e.

$$R_O = < (R_{\rm MIN} + R_{\rm MAX})/2 >, \quad (1)$$

where the brackets $<>$ further represent a time average over Δt, which is the time delay from the first sighting (t_{EN}, the time of the front boundary crossing) to the rear boundary (at t_{EX}, the exit crossing), i.e. $\Delta t = t_{EX} - t_{EN}$, where the clock starts when the MC lifts off the Sun. (Notice then that t_{EN} is just the Sun-to-Earth travel time for the MC.) So Δt in this case is identified as T, the duration of the spacecraft passage through the MC, and sometimes simply called "duration". We acknowledge that the approximation in Eq. (1) is usually a source of error in our estimates of V_E, but not usually a significant one in the vector method.

3.1 The scalar derivation of V_E

We start with the formulation of the "**s**calar derivation" of V_E. Farrugia et al. (1992a, b) show that

$$V_{E,S} = r_O (t_{EN} + \Delta t)^{-1}, \quad (2)$$

where all quantities are measured in a frame of reference where the MC's average velocity is zero, and where r_O is the radius of the MC as initially observed at the MC's front boundary at time t_{EN} (at 1 AU in our case). Simply put, this formula is derived from the fact that a relatively small structure, the MC at the Sun, must expand when going from the Sun to Earth, since its cross-section is observed to be a large fraction of an AU at 1 AU, and it was further assumed that it does so uniformly at constant speed over 1 AU. Next we assume that the average speed from the Sun to Earth ($<V_{\rm S-to-E}>$) is almost the same as the average speed $<V_C>$ of the plasma within the MC, as observed at 1 AU. Hence,

$$< V_{\rm S-to-E} > \approx < V_C > . \quad (3)$$

(We assume that Eq. (3) holds, even though it has been established that there is some acceleration or deceleration of ejecta generally (see, e.g. Gopalswamy, 2000), since this apparently occurs mainly near the Sun, and therefore does not negate the good approximation of Eq. (3).) Then

$$<V_{\rm S-to-E}> t_{EN} \approx < V_C > t_{EN} \approx 1\,{\rm AU},$$

or

$$t_{EN} \approx 1\,{\rm AU}/ < V_C > . \quad (4)$$

Hence, from Eqs. (2) and (4), we see that

$$V_{E,S} \approx (R_O < V_C > /1\,{\rm AU})(1 + T < V_C > /1\,{\rm AU})^{-1}, \quad (5)$$

where we identify r_O as approximately R_O. As mentioned above and confirmed here, $V_{E,S}$ depends on MC duration, speed, and size, all scalars. We now check $V_{E,S}$ for reasonableness by using typical values, for a low speed MC case, on the right side of Eq. (5), i.e. by using values such

as R_O=0.125 AU, $<V_C>$=450 km/s, T=20 h; see e.g. Lepping et al. (2006) which provides these average values. This gives $V_{E,S}$=46 km/s, which is within a typical range of values for the MC expansion speed at 1 AU for the slower MCs (see, e.g. Lepping et al., 2002). For MCs moving at, say, 650 km/s and keeping all other values in Eq. (5) the same, we obtain a $V_{E,S}$ of 62 km/s. Both of these are markedly lower (by a factor of about two) than the value of 114 km/s derived by Burlaga (1995, p. 100) for the expansion speed of a particular case (14/15 January 1988) under somewhat similar circumstances.

3.2 The vector derivation of V_E

We now provide the "**v**ector derivation" of the expansion velocity, called $V_{E,V}$, which will depend on the gradient of the speed across the MC (i.e. strictly on the component $V_{Z,\mathrm{CL}}$ across the part of the MC where the gradient is smoothest and steepest), so it depends strictly on local and relevant measured plasma velocities after coordinate transformation and to some extent on MC modeling results, but to a lesser degree.

Figure 1 shows the portions of the $|V_{Z,\mathrm{CL}}|$ profile (in black and red dashed lines) that may be used for finding the "gradient" of $|V_{Z,\mathrm{CL}}|$ across the MC; actually only a vector difference will be used, not the gradient itself. The MC expansion is assumed to be perpendicular to the MC axis, i.e. 2-D, and further it is assumed to be isotropic. The three panels below $|V_{Z,\mathrm{CL}}|$ (in which green curves are shown) in Fig. 1 give profiles of the magnetic field (magnitude and latitude angle, in a GSE system, for example) and proton plasma beta that are commonly seen in interplanetary MCs at 1 AU, in order to put the associated change in $|V_{Z,\mathrm{CL}}|$ in context. As Fig. 1 is meant to indicate, and we stress here, there are two distinct types of $|V_{Z,\mathrm{CL}}|$-profiles, where the maximum (MAX) and minimum (MIN) values occur at the boundaries (the black curve) or somewhere within those boundaries (the red dashed curve). We will treat each type separately below, but first we give a few examples of expanding MCs.

Figure 2 shows six examples of speed (V=$|\boldsymbol{V}|$) profiles, emphasizing the gradient of plasma velocity, as the WIND spacecraft passes through a MC that is expanding. Also shown are the magnetic field magnitude ($\boldsymbol{B}$), and field latitude angle (θ, in GSE coordinates). Black solid vertical lines indicate the identified start and end times of the MC, as given by Lepping et al. (2006) and depend only on magnetic field quantities; dotted vertical (blue) lines indicate identifications, made through visual inspection, of the positions of MAX and MIN in the speed profile; and dashed (red) vertical lines are points of MAX and MIN chosen automatically, as described in Fig. 2's caption. (a) is the MC with start day of 4 February 1998, (b) is for 8 November 1998, (c) is for 21 February 2000, (d) is for 22 April 2001, (e) is for 29 April 2001, and (f) is for 15 May 2005. We note that the average speeds for these MCs range from 323 km/s (a) to 880 km/s (f), and this average is the same, or almost the same, regardless of whether the average was taken over the full MC or over only $\Delta t'$ (giving $<V'>$; only case (f) shows any noticeable difference. However, the ΔVs (and the $\Delta|V_Z|$s, discussed later) can differ significantly between the black and red (taken over $\Delta t'$) type of averages; note especially case (f) where ΔV is 149 km/s (black) and the other (red) is 229 km/s. In almost all cases the red cases of ΔV are larger than the black, and for the one exception (case e) the two quantities are close in value. Notice also that these six examples cover almost all major "types" of MCs as described by Lepping and Wu (2007), where two (cases b and d) have nearly a full interval of southward field, two other cases (c and f) are nearly all northward, and remaining two (cases a and e) are about half northward and half southward. Most important is the fact that the velocity gradients usually come close to covering the full MCs. In fact, in case (e) all three types of gradient end-points are in very close agreement. Only in case (f) is there dramatic disagreement in the position of the vertical lines, in the front region; even for this case the end of the gradient shows remarkable agreement for the three estimates. Front vs. rear disagreement is evenly divided among these six examples. In three cases we see that the speed reaches a minimum several hours before the estimated rear boundary of the MCs; these are cases (b), (c), and (d). This is apparently due to the increased speed of the external plasma ramming into the MCs. This phenomena was first pointed out by Lepping et al. (2003b) where the superposition of many MCs were used to find this peculiar feature that occurs for many, but not all, MCs.

As the cases in Fig. 2 exemplify, the V-profile within a MC is not always simple or well behaved, and since $|V_Z|$ (now understood to be in CL coordinates) is directly related to V (as discussed in Sect. 2), we will translate this assessment directly to the component $|V_Z|$. For example, $|V_Z|$ is not always smoothly decreasing from spacecraft entrance to exit and, even when $|V_Z|$ does smoothly change in time, the MAX and MIN of $|V_Z|$ are not always at the entrance and exit points, respectively, as was briefly discussed for Fig. 1. Hence, we found it necessary to filter the $|V_Z|$ values by use of a running average of 2-h length, slipped every minute, to find the maximum value of $|V_Z|$ ($|V_{Z,\mathrm{MAX}}|$) and the minimum value of $|V_Z|$ ($|V_{Z,\mathrm{MIN}}|$), on the basis of initially one minute "sample rate" data. This was done in order to obtain the low frequency variation of $|V_Z|$ for analysis. From these filtered-$|V_Z|$ values, we find the MAX and MIN values, and from 15-min averages (from the smoothed 1-min averages) centered on the MAX and MIN positions. This approach will be utilized below in one way of finding $V_{E,V}$. In another approach, we use the closest 15-min averages of $|V_Z|$ to the boundaries. In both approaches we decrease any possible errors due to peculiar noise-fluctuations in $|V_Z|$ (that is unrelated to the actual measure of the gradient) either at the boundaries or at MAX and/or MIN. In this way, any damage due to noise-fluctuations is at least minimized.

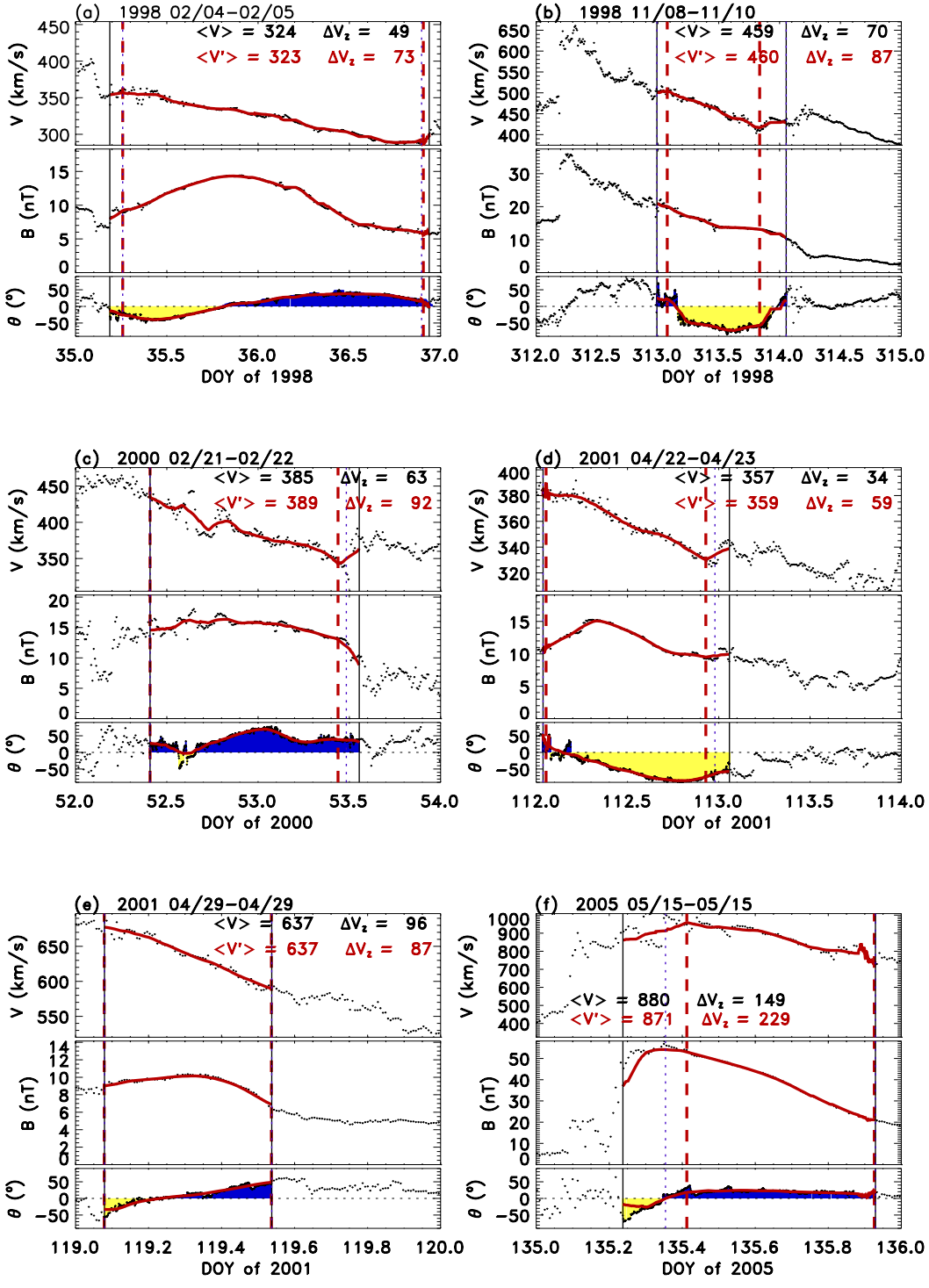

Fig. 2. Six examples of the profiles of plasma speed (V=|**V**|), magnetic field magnitude ($\boldsymbol{B}$), and field latitude angle (θ) as the WIND spacecraft passes through a MC. All data presented in 10-min average form. Black solid vertical lines indicate the identified start and end times of the MC; dotted vertical (blue) lines indicate choices, through visual inspection, of the points of MAX and MIN in the speed profile; and dashed (red) vertical lines are points of MAX and MIN chosen automatically, via computer searching, after V is smoothed via a running average of 2 h length. Average speed is given in the V-panel, as $<V>$ for an average over the full MC and as $<V'>$ (in red) for the $\Delta t'$ region, both in units of km/s. Panels (a) through (f) are ordered according to date: **(a)** is the MC with start day of 4 February 1998, **(b)** is for 8 November 1998, **(c)** is for 21 February 2000, **(d)** is for 22 April 2001, **(e)** is for 29 April 2001, and **(f)** is for 15 May 2005. In each θ-panel the regions where the magnetic field goes southward are in yellow and when northward they are in blue.

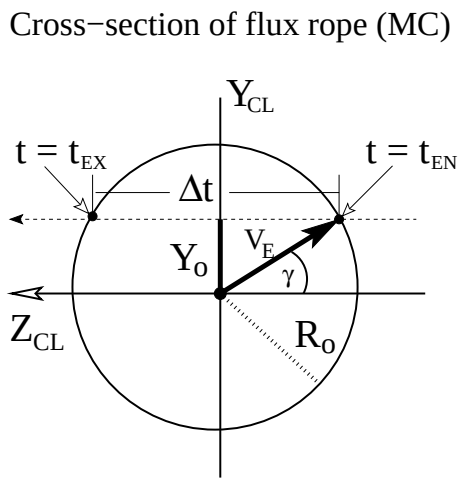

Fig. 3. The cross-section of an ideal MC (circular for convenience) where the spacecraft passes at a closest approach distance Y_O from the axis, where t=t_{EN} is the entrance time and t=t_{EX} is the exit time; these times are separated by Δt=T, the "duration" of time that the spacecraft spends inside the MC. $\mathbf{V}_E$ is the expansion velocity perpendicular to the MC's axis and shown for the entrance time, t_{EN}. The magnitude of $\mathbf{V}_E$ ideally holds for all γ angles.

Figure 3, which shows the cross-section of the ideal MC (circular for convenience) giving the relationship of expansion speed V_E (moving out radially from the axis) and the velocity of the internal plasma relative to the motion of the center of the MC. Figure 3 indicates the passage of the spacecraft from the initial contact point, where the velocity is $\mathbf{V}_{EN}$, to the exit point where the velocity is $\mathbf{V}_{EX}$ occurring over time Δt=T. As pointed out above, the relevant velocity-gradient of interest is that of the Z-component as rendered in CL coordinates (as in Fig. 1). The MC's **c**enter-velocity can be thought of as the average across the MC, called $<\mathbf{V}_C>$, taken along the spacecraft's path; this is hopefully a good approximation, since the spacecraft does not usually go exactly through the MC's center. This average is transformed to CL coordinates to give $<\mathbf{V}_C>_{\rm CL}$, and the $Z_{\rm CL}$-component obtained, called $<V_Z>_{\rm CL}$. We then form $\Delta V_{Z,EN,{\rm CL}}$=$(V_{Z,EN}-<V_Z>)_{\rm CL}$ (for inbound compared to average) and $\Delta V_{Z,EX,{\rm CL}}$=$(V_{Z,EX}-<V_Z>)_{\rm CL}$ (for outbound compared to average), where $|V_{Z,EN,{\rm CL}}|$ is the $Z_{\rm CL}$-component of velocity of the MC's plasma usually near $|V_{Z,{\rm MAX,CL}}|$, and $|V_{Z,EX,{\rm CL}}|$ is the $Z_{\rm CL}$-component of velocity usually near $|V_{Z,{\rm MIN,CL}}|$, both in an inertial frame of reference. Hence, $\Delta V_{Z,EN,{\rm CL}}$ and $\Delta V_{Z,EX,{\rm CL}}$ are the $V_{Z,{\rm CL}}$-components of the MC's boundary velocities, essentially "inbound" and "outbound," respectively, in the MC's moving reference frame (with the average speed), in CL coordinates. We then form the difference between these two differences

$$\Delta(\Delta V_Z)_{\rm CL} = (|\Delta V_{Z,EN}| - |\Delta V_{Z,EX}|)_{\rm CL}, \quad (6)$$

which is the $Z_{\rm CL}$-component of the velocity difference the across the MC. We choose $\Delta(\Delta V_Z)_{\rm CL}$ to be positive in all cases (as well as both $|\Delta V_{Z,EN,{\rm CL}}|$ and $|\Delta V_{Z,EX,{\rm CL}}|$ individually), where there is actual expansion. And since $\boldsymbol{Z_{\rm CL}}\cdot\mathbf{1}_{\mathbf{X},{\rm GSE}}$ is always negative, we must use absolute values in Eq. (6).

From Fig. 3 it is ascertained that

$$V_{E,V}\cos\gamma = \Delta(\Delta V_Z)_{\rm CL}/2, \quad (7)$$

where the factor of 2 arises from the fact that $\Delta(\Delta V_Z)_{\rm CL}$ itself is twice the horizontal projection of the expansion speed, since values were taken at the two boundaries, rather than one at the center and the other at one of the boundaries. Since Z_O^2+Y_O^2=R_O^2, and cosγ=$\sqrt{(Z_O^2/R_O^2)}$=$\sqrt{(1-Y_O^2/R_O^2)}$, as also seen in Fig. 3, then

$$\begin{aligned} V_{E,V} &= \Delta(\Delta V_Z)_{\rm CL}/2\cos\gamma \\ &= \Delta(\Delta V_Z)_{\rm CL}/(2\sqrt{(1-Y_O^2/R_O^2)}), \end{aligned}$$

or

$$V_{E,V} = \Delta(\Delta V_Z)_{\rm CL}/(2\sqrt{(1-|CA|^2)}), \quad (8)$$

where |CA|≡$|Y_O|/R_O$, is the relative closest approach parameter.

It is important to point out that the gradient of velocity within most MCs tends to be greatest in the central regions of the MCs, i.e. the points of $|V_{Z,{\rm MAX,CL}}|$ and $|V_{Z,{\rm MIN,CL}}|$ generally are not exactly at the boundaries of the MC. It appears that the times of $|V_{Z,{\rm MAX,CL}}|$ and $|V_{Z,{\rm MIN,CL}}|$ (i.e. $t_{\rm MAX}$ and $t_{\rm MIN}$, respectively), are the proper places to estimate the values of velocity to use in our vector formulation, since a gradient that is calculated based on velocities at the times of the actual MC boundaries (and using real duration) is often much smaller than a realistic one, as a broad review of many MCs reveals. We believe that the proper gradient then is $\Delta V_{Z,{\rm CL}}/\Delta t'$, where $\Delta t'$ is determined by using the difference between the times of $|V_{Z,{\rm MAX,CL}}|$ and $|V_{Z,{\rm MIN,CL}}|$, i.e. $\Delta t'$=$t_{\rm MIN}-t_{\rm MAX}$; see Fig. 1 which gives the pictorial representation of $\Delta t'$. This is the portion of the MC where expansion is actually occurring and apparently would be so throughout the MC, if it were not for front and rear interaction with the solar wind. Hence, with this consideration Eq. (8) becomes

$$V'_{E,V} = \Delta(\Delta V_Z)'_{\rm CL}/(2\sqrt{(1-|CA|^2)}), \quad (9)$$

where $\Delta(\Delta V_Z)'_{\rm CL}$ is now understood to be based on

$$\Delta(\Delta V_Z)'_{\rm CL} = (|\Delta V_{Z,{\rm MAX}}| - |\Delta V_{Z,{\rm MIN}}|)_{\rm CL}, \quad (10)$$

i.e. based on $|V_{Z,{\rm MAX,CL}}|$, $|V_{Z,{\rm MIN,CL}}|$, separated by $\Delta t'$. We assume that Eq. (9) will usually be the proper means of estimating vector velocity expansion, and it will be used for that estimate. But for comparison, we will also estimate expansion based on Eq. (8), understanding that it is almost always going to give a lower bound to the estimate. And, of course, our assumption will be tested.

Finally, we should stress that it is clear that the positions where $|V_{Z,\mathrm{MAX,CL}}|$ and $|V_{Z,\mathrm{MIN,CL}}|$ occur should not be considered to be indicators of the MC boundaries, in any case, because many other physical indicators are much better at determining MC boundaries, e.g. changes in $|\mathbf{B}|$, proton temperature, proton plasma beta, direction of $\mathbf{B}$, and indications from model fitting, etc.; see Lepping and Wu (2007). And, as expected from what we have said above, those other (reliable) quantities often disagree, even if only slightly, with using velocity as a means of determining the boundary. Even when velocity does appear to agree with these other means, its change is usually not sharp enough, at the start or end of the gradient, to pin down very well the time of occurrence of the boundary. As we see, Eqs. (8) and (9) depend on the Z_{CL} component of a velocity change, and on the relative closest approach (which depends on Y_O, the magnitude of the closest approach vector).

We now check $V'_{E,V}$ for reasonableness by using typical values on the right side of Eq. (9), such as $\Delta(\Delta V_Z)'_{\mathrm{CL}}$=60 km/s, R_O=0.125 AU, and Y_O=0.05 AU. This gives $V'_{E,V}$=33 km/s, which, like $V_{E,S}$ (test), is within a typical range of values for the MC expansion speed at 1 AU, especially for the slower moving MCs. But it appears that using $V'_{E,V}$ is generally going to give lower estimates of V_E than using $V_{E,S}$, and using $V_{E,V}$ (as in Eq. 8), on average, is expected to give even slightly lower values than $V'_{E,V}$.

4 The data and results

Most of the 100 MCs initially considered in this study (i.e. 82 of them) are parameter fitted and discussed by Lepping et al. (2006), based on data from WIND/MFI (Lepping et al., 1995) and WIND/SWE (Ogilvie et al., 1995). The start/end times of the full 100 MCs, along with their various derived and estimated characteristics are provided on the WIND/MFI Website with URL of http://lepmfi.gsfc.nasa.gov/mfi/mag_cloud_S1.html and referred to as Table 2 on that site. Of these only MCs of relatively good quality were used, meaning the MCs that possess quality indices of Q_O=1,2 (where Q_O=3 is poor), where Q_O depends on the following MC parameters: the value of the chi-squared of the parameter fit, a comparison of two independent means of estimating the MC's radius, where only one means depends on $\Delta t'$ (or on duration, T), the value of closest approach (CA) distance, reasonableness of the estimated diameter ($2\,R_O$), reasonableness of profile-symmetry, comparison of the MC axis alignment to what an axis in the MC's flanks (viewed globally) would be, and a check of the sign/strength of the axial-field component in the CL coordinate system. (See Appendix A of Lepping et al., 2006, for a rigorous definition of Q_O). After this quality editing the set of N=100 MCs is reduced to N'=64 cases. The reason for restricting our analyses to those of quality Q_O=1,2 is because, as we saw, certain model quantities and abilities are required in our estimation of V_E, such as R_O, Y_O, (and indirectly T), and being able to accurately transform into the CL coordinate system which requires obtaining accurate estimates of the latitude and longitude of the MC's axis. The N'=64 cases were individually inspected to see if there was a gradient across each MC, or across a major part of it, indicating that the MC is, indeed, expanding at the time of the observations. Another 11 cases were dropped because they did not have such a gradient, i.e. they were not good cases of expanding MCs where both $\Delta(\Delta V_Z)_{\mathrm{CL}}$ and $\Delta(\Delta V_Z)'_{\mathrm{CL}}$ were positive. Hence, we arrive at N=53 good cases for analysis. So a high percentage, 83%, of the eligible 64 cases were actually expanding.

Table 1 shows, for the full 53 MCs, the start time, duration (T), $\Delta t'$, R_O, |CA|, and various relevant speeds and velocity components, needed for use in Eqs. (5), (8) and (9), including $<V_C>$, the difference quantities, $\Delta(\Delta V_Z)_{\mathrm{CL}}$ for both conditions (MAX/MIN) and for the boundaries, and the last three columns provide the estimates of expansion speed: $V_{E,S}$, $V_{E,V}$, and $V'_{E,V}$, in that order; all quantities are defined in the footnotes. At the bottom, in red, are the averages and standard deviations (σ) for each quantity. It is clear that $V_{E,S}$ ($\equiv V^n$ in Table 1) is on average (as well as for most individual cases) closer to $V'_{E,V}$ ($\equiv V^p$) than to $V_{E,V}$ ($\equiv V^o$). Also there is a relatively small spread of $V_{E,S}$ values (with a σ=27 km/s) compared to its average (49 km/s), i.e. a ratio ($\equiv$avg/σ) of 0.55. This is especially so with regard to that ratio for $V_{E,V}$, which is 1.06, or for $V'_{E,V}$, which is 0.86. In the four cases where $V_{E,S}$ was unusually large, say over 85 km/s, $V_{E,V}$ and $V'_{E,V}$ were also very large. This is very noticeable in the case where $V_{E,S}$ is largest (i.e. case 2001, 11, 24); there we see that $V_{E,S}$=151 km/s, $V_{E,V}$=262 km/s, and $V'_{E,V}$=213 km/s, but in this case the latter two (although clearly being very large) are not very believable. In Fig. 4 we show a scatter diagram of $V_{E,S}$ vs. $V_{E,V}$, based on the values in Table 1, with a least-squares fitted straight line; the c.c. for this correlation is 0.76. So as $V_{E,V}$ increases so also does $V_{E,S}$, and the correlation is more-or-less linear. It is interesting that the majority of the values for $V_{E,V}$ lie between 5 and 70 km/s, and for $V_{E,S}$ they are mainly within 10 and 80 km/s, as Table 1 reveals. We now investigate the distributions of the $V_{E,S}$ and $V_{E,V}$ values.

Figure 5 shows histograms of the values derived for $V_{E,S}$ (black solid line) and $V_{E,V}$ (red dashed line) based on Eqs. (5) and (8), respectively. The peaks for both are at 30 km/s (with bucket widths of 20 km/s), and the averages and standard deviations (σ) are shown for the two sets. Note that both distributions are skewed, so that the average value for $V_{E,V}$ is higher than its most probably value (30 km/s), and for $V_{E,S}$ the average is quite a bit higher than its most probable value (also 30 km/s). In fact, as pointed out above, there is one value of $V_{E,V}$ as high as 263 km/s (not shown in the histogram). There is obviously larger uncertainty on this large estimate, calling in doubt the fact that it is actually so high, but it is likely that there are some actual expansion velocities much higher than 30 km/s; see Burlaga (1995, p. 100).

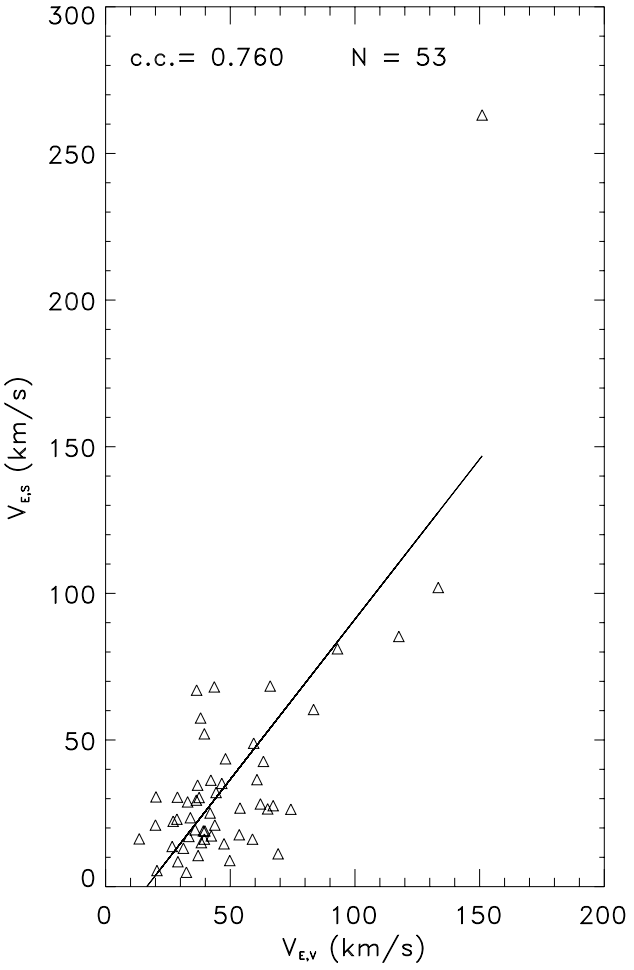

Fig. 4. A scatter diagram of $V_{E,S}$ vs. $V_{E,V}$ showing a linear correlation coefficient (c.c.) of 0.76. (Note that there is one value of $V_{E,V}$ of 263 km/s that occurs off-scale and therefore is not shown. This value was included in the least-squares fit and in the calculation of c.c., however.)

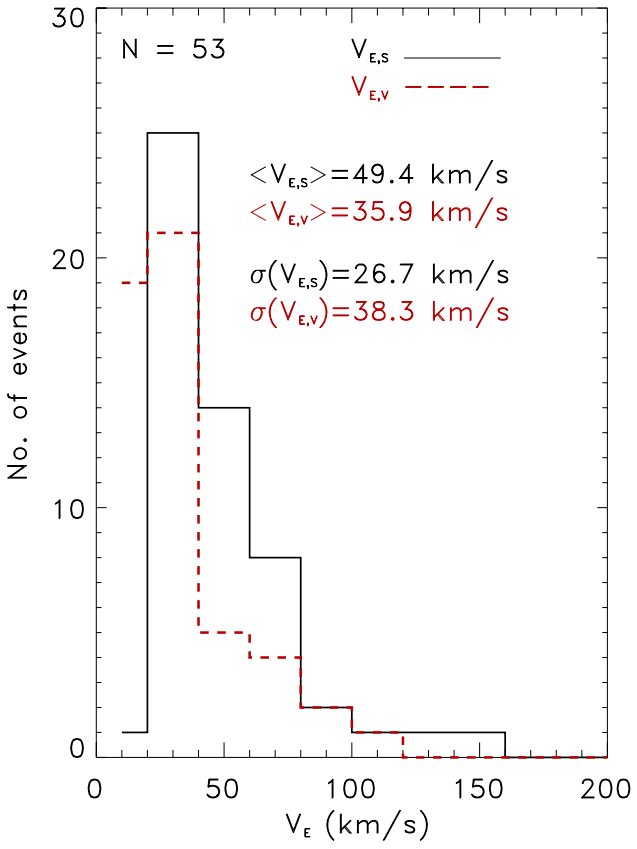

Fig. 5. Histograms of the values derived for $V_{E,S}$ (black) and $V_{E,V}$ (in red) based on Eqs. (5) and (8), respectively, i.e. where the latter is based on the actual boundary values of V_Z of the MCs. The peaks for both are at 30 km/s for bucket widths of 20 km/s and the averages and standard deviations (σ) are shown for the two sets. (Note that there is one value of $V_{E,V}$ of 263 km/s that occurs off-scale and therefore is not shown.)

Figure 6 is a scatter plot of $V_{E,S}$ vs. $V'_{E,V}$, which is similar to that of Fig. 4, except $V_{E,V}$ of Fig. 4 is replaced by $V'_{E,V}$ in Fig. 6; notice, however, that the scales are also different. As we see, there are similarities in the values in the two figures, but the c.c.'s are significantly different, i.e. c.c.=0.85 and 0.76 for Figs. 6 and 4, respectively. This improvement in correlation is not unexpected, since we postulated that the MAX/MIN means was expected to give a more faithful representation of the gradient of velocity across the MC (and therefore better represent expansion) than the boundary value means. We now investigate the distributions of the values $V'_{E,V}$ and again show $V_{E,S}$ for comparison.

Figure 7 shows histograms of the values derived for $V_{E,S}$ (black solid line) and $V'_{E,V}$ (red dashed line) based on Eqs. (5) and (9), respectively; $V_{E,S}$ is again shown for comparison. The peaks for both are at 30 km/s (with bucket widths of 20 km/s) and the averages and standard deviations (σ) are shown for $V_{E,V}$: $<V'_{E,V}>$=44 km/s and $\sigma(V'_{E,V})$=38 km/s (the comparable values for $<V_{E,S}>$ are given in Fig. 5). Note that both distributions are skewed, so that the averaged value for $V'_{E,V}$ is higher than its most probably value (30 km/s), and again for $V_{E,S}$ ($<V_{E,S}>$=49 km/s) the average is quite a bit higher than its most probable value (30 km/s), as discussed in connection with Fig. 5. There is obviously larger uncertainty on the very high values, e.g. those above 100 km/s, again calling into doubt that they are really so high.

5 Estimates of errors

For the scalar determination of V_E, which depends on R_O, $<V_C>$, and T, the net error on V_E results from the combined errors from each of these three quantities. The error on R_O is greatest, since $<V_C>$ and T are generally quite well

Table 1. Magnetic cloud parameter values.

Start time				T^a	$\Delta t'^b$	R_O^c	CA^d	V^e	V^f	V^g	V^h	V^i	V^j	V^k	ΔV^l	ΔV^m	V^n	V^o	V^p
Year	M	D	H	(Hours)		(AU)		(Km/s)											
1995	02	08	5.8	19.0	13.7	0.108	0.49	407	401	411	427	408	427	379	19	47	37	11	27
1995	04	03	7.8	27.0	17.6	0.152	0.71	300	299	294	338	257	336	261	81	75	38	58	53
1995	08	22	21.3	22.0	15.6	0.126	0.48	359	358	357	371	342	374	343	29	31	40	16	18
1996	05	27	15.3	40.0	31.6	0.175	0.11	368	333	368	374	345	373	310	29	62	48	15	31
1996	07	01	17.3	17.0	16.4	0.086	0.16	353	353	352	368	341	364	339	27	25	27	14	13
1996	08	07	12.3	22.5	9.6	0.106	0.46	345	338	347	351	343	352	333	9	19	32	5	11
1996	12	24	2.8	32.5	32.4	0.143	0.47	349	347	349	398	306	405	309	92	95	40	52	54
1997	01	10	5.3	21.0	17.0	0.095	0.11	437	402	440	427	381	427	379	47	48	34	24	24
1997	06	09	2.3	21.0	9.0	0.093	0.53	373	240	370	244	229	253	222	15	32	29	9	19
1997	07	15	8.8	15.0	11.2	0.064	0.00	364	359	364	362	352	369	339	11	30	21	6	15
1997	09	22	0.8	16.5	14.9	0.117	0.03	419	375	414	407	334	423	331	73	92	42	36	46
1997	10	01	16.3	30.5	28.9	0.198	0.44	451	355	451	377	328	375	325	50	50	67	28	28
1997	10	10	23.8	25.0	23.6	0.114	0.57	397	397	396	429	373	428	368	57	60	37	35	37
1997	11	07	15.8	12.5	7.8	0.110	0.16	423	394	416	405	371	413	371	34	42	42	17	21
1997	11	08	4.9	10.0	4.8	0.058	0.48	385	359	382	376	322	368	340	54	28	20	31	16
1998	01	07	3.3	29.0	24.0	0.119	0.02	381	327	385	352	313	351	302	39	49	36	19	25
1998	02	04	4.5	42.0	39.5	0.147	0.89	324	321	323	354	293	354	281	61	73	37	67	80
1998	03	04	14.3	40.0	35.3	0.163	0.06	344	303	347	334	292	337	275	42	62	44	21	31
1998	06	02	10.6	5.3	4.3	0.035	0.20	400	385	399	398	366	390	375	32	15	14	16	8
1998	06	24	16.8	29.0	21.7	0.104	0.23	461	266	466	308	279	303	235	29	69	38	15	35
1998	08	20	10.3	33.0	24.5	0.107	0.13	317	305	311	320	276	330	278	44	53	27	22	27
1998	09	25	10.3	27.0	27.0	0.204	0.57	645	521	645	594	460	609	462	133	147	93	81	90
1998	11	08	23.8	25.5	18.2	0.123	0.16	459	451	461	489	426	495	409	63	86	44	32	43
1999	08	09	10.8	29.0	27.9	0.135	0.26	342	331	343	367	308	366	311	59	54	38	30	28
2000	02	21	9.8	27.5	24.7	0.134	0.22	386	375	389	423	374	421	331	49	89	42	25	46
2000	08	12	6.1	23.0	20.2	0.142	0.01	577	575	580	637	581	639	526	57	113	62	28	57
2000	10	03	17.1	21.0	12.1	0.092	0.23	409	366	406	377	351	379	350	26	29	31	13	15
2000	10	13	18.4	22.5	21.8	0.119	0.11	400	300	400	314	276	311	288	38	23	39	19	12
2000	11	06	23.1	19.0	14.7	0.138	0.19	536	490	526	514	418	537	420	96	117	59	49	60
2001	03	19	23.3	19.0	16.0	0.083	0.19	411	296	411	322	277	323	277	45	46	29	23	23
2001	04	04	20.9	11.5	9.7	0.191	0.86	734	721	727	765	677	767	666	87	100	118	85	98
2001	04	12	7.9	10.0	3.7	0.124	0.68	636	401	632	435	419	415	389	16	26	69	11	18
2001	04	22	0.9	24.5	21.0	0.132	0.05	357	357	360	382	344	389	329	38	60	40	19	30
2001	04	29	1.9	11.0	11.0	0.116	0.39	638	580	638	618	539	616	536	79	80	63	43	43
2001	05	28	11.9	22.5	22.5	0.125	0.37	457	352	457	389	323	388	323	66	65	47	35	35
2001	07	10	17.3	39.5	24.4	0.127	0.51	350	331	352	365	335	364	312	29	52	33	17	30
2001	10	31	21.3	37.0	24.0	0.140	0.09	337	329	342	369	310	375	304	59	71	36	30	36
2001	11	24	15.8	21.5	19.8	0.280	0.80	737	730	730	943	627	880	625	316	255	151	263	213
2002	03	24	3.8	43.0	19.3	0.215	0.08	437	423	435	458	405	455	395	53	60	65	27	30
2002	04	18	4.3	22.0	22.0	0.159	0.53	480	360	480	403	341	390	336	62	54	61	37	32
2002	05	19	3.9	19.5	15.8	0.212	0.95	460	446	456	453	415	472	405	38	67	83	60	107
2002	08	02	7.4	13.7	13.2	0.127	0.11	493	448	494	473	419	474	423	53	51	54	27	26
2003	08	18	11.6	16.8	9.5	0.144	0.12	487	461	471	460	428	511	395	32	117	59	16	59
2003	11	20	10.8	15.5	13.4	0.090	0.03	594	583	606	677	541	690	511	136	178	44	68	89
2004	04	04	2.8	36.0	28.4	0.197	0.48	431	439	436	519	399	515	379	120	136	66	68	77
2004	07	24	12.8	24.5	12.8	0.177	0.30	551	549	546	578	527	587	491	50	96	74	26	50
2004	11	08	3.4	13.2	10.5	0.086	0.27	684	504	681	485	468	534	468	17	67	50	9	35
2004	11	10	3.6	7.5	7.5	0.075	0.41	730	665	730	706	626	710	624	80	86	48	44	47
2005	05	15	5.7	16.6	12.3	0.195	0.75	879	881	871	878	743	958	729	135	230	133	102	174
2005	05	20	7.3	22.0	14.2	0.090	0.34	456	420	446	437	382	444	387	54	57	33	29	30
2005	06	12	15.6	15.5	11.3	0.131	0.28	483	433	486	458	424	451	415	34	36	54	18	19
2005	07	17	15.3	12.5	10.3	0.074	0.44	426	426	428	455	400	445	399	55	46	29	31	25
2006	02	05	19.1	18.0	18.0	0.068	0.01	340	335	340	350	308	354	307	42	47	20	21	24
Average				22.6	17.7	0.130	0.33	458	417	457	449	391	453	381	58	72	49	36	44
σ				9.2	8.1	0.046	0.25	128	125	127	140	109	143	107	47	48	27	38	38

Footnotes on next page.

Table 1. Continued.

[a] T is the duration in hours
[b] $\Delta t'$ is the interval between the points at $V_{\rm MAX}$ and $V_{\rm MIN}$ in hours
[c] R_O is the estimated radius of the MC, which is $\approx<(R_{\rm MIN}+R_{\rm MAX})/2>$
[d] |CA| is the relative closest approach distance = $|Y_O|/R_O$ (in %)
$V^{\rm e} = <V_C>$ is the average (over T) speed of the MC locally
$V^{\rm f} = <|V_{Z,{\rm CL}}|>$ is the average of absolute value ("ABS") of the Z-component of the velocity across the full MC
$V^{\rm g} = <|V'_{Z,{\rm CL}}|>$ is the average of ABS of Z-component of the velocity across $\Delta t'$
$V^{\rm h} = |V_{Z,{\rm MAX,CL}}|$ is ABS of the Z-component of the velocity at the maximum-point in CL coords.
$V^{\rm i} = |V_{Z,{\rm MIN,CL}}|$ is the ABS of Z-component of the velocity at the minimum-point in CL coords.
$V^{\rm j} = |V_{Z,O,{\rm CL}}|$ is the ABS of Z-component of the velocity at the MC entrance-point in CL coords.
$V^{\rm k} = |V_{Z,EX,{\rm CL}}|$ is the ABS of Z-component of the velocity at the MC exit-point in CL coords.
$\Delta V^{\rm l} = \Delta(\Delta V_Z)_{\rm CL}$ is the equal to ($|V_{Z,O,{\rm CL}}| - |V_{Z,EX,{\rm CL}}|$), i.e. the difference value of the Z-velocity component between the entrance and exit points. Equation (6) is equivalent to this.
$\Delta V^{\rm m} = \Delta(\Delta V_Z)'_{\rm CL}$ is equal to ($|V_{Z,{\rm MAX,CL}}| - |V_{Z,{\rm MIN,CL}}|$), i.e. the difference value of the Z-velocity component between the MAX and MIN points. Equation (10) is equivalent to this.
$V^{\rm n} = V_{E,S}$ is the scalar estimate of expansion speed based on $<V_C>$ and T
$V^{\rm o} = V_{E,V}$ is the vector estimate of expansion speed based on $|V_{Z,O,{\rm CL}}|$, $|V_{Z,EX,{\rm CL}}|$ and T
$V^{\rm p} = V'_{E,V}$ is the vector estimate of expansion speed based on $|V_{Z,{\rm MAX,CL}}|$, $|V_{Z,{\rm MIN,CL}}|$ and $\Delta t'$

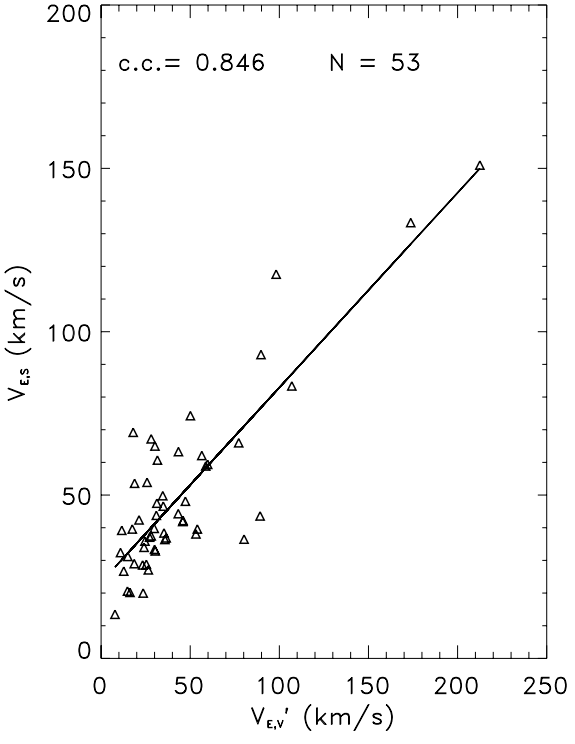

Fig. 6. A scatter diagram of $V_{E,S}$ vs. $V'_{E,V}$ showing a c.c. of 0.85.

determined. The sources of error in R_O are: (1) it is model-dependent with all of the model's sources of errors and (2) a simple value for R_O ($\approx<(R_{\rm MIN}+R_{\rm MAX})/2>$) may not be adequate for a MC with an oval cross-section, as briefly discussed in the beginning of Sect. 3. But as we will see the structure of Eq. (5) is such that it propagates errors most seriously for large errors in T, not so much for R_O. Here we attempt to estimate the typical impact of these errors. First, we will assume that: (1) $<V_C>$ is well known and essentially error free (or very small compared to the errors of the other two quantities), (2) T is known to an uncertainty of 10%, (3) the assumption that the average speed across the MC, $<V_C>$, is approximately equal to $<V_{\rm S-to-E}>$ (Eq. 3) is a very good one, and (4) R_O is known to an uncertainty of about 30%. Hence, using the example at the end of Sect. 3.1, where T is 20 h and R_O is 0.125 AU, and where two values of $<V_C>$ were used, 450 km/s and 650 km/s, we see that these uncertainties yield these specific ranges for the three relevant quantities: $<V_C>$=450 km/s, R_O: (0.0875–0.163) AU, and T: (18–22) h. Then from Eq. (5) and for $<V_C>$=450 km/s we obtain for the MAX value $V_{E,S}$=61.3 km/s and a MIN value of 31.8 km/s, or $V_{E,S}$ is 47±15 km/s. But for a MC moving on average at $<V_C>$=650 km/s we obtain $V_{E,S}$ to be 63±20 km/s. As we see, the error is dominated by the error on T which is usually fairly small. However, the assumption that $<V_C>\approx<V_{\rm S-to-E}>$ may not be good in all cases. For example, if there were a marked deceleration of a MC (which is believed to occur occasionally near the Sun), then this assumption may not be very good, and therefore, be another source of error, one not easily estimated. Therefore, any estimated error on $V_{E,S}$, as done above, must be considered a minimum estimate.

For the vector determination of V_E, which depends on R_O and Y_O, (giving $|{\rm CA}|\equiv|Y_O|/R_O$), and on the difference-velocity $\Delta(\Delta V_Z)'_{\rm CL}$ (where we recall that the prime refers to obtaining the difference from the MAX and MIN components of velocity). This difference-velocity, obtained

straightforwardly from measurements, should be quite well determined, but not completely error-free. Both $|Y_O|$ and R_O are sources of error, especially Y_O, which is, unfortunately, one of the most poorly estimated quantities in the Lepping et al. (1990) fitting program; see Lepping et al. (2003a). However, the structure of Eq. (8) is such that the net error in V_E will not depend strongly on the error in |CA|, as we will see. Here we attempt to estimate the typical impact of these two errors (in |CA| and $\Delta(\Delta V_Z)'_{\rm CL}$). The error in $\Delta(\Delta V_Z)'_{\rm CL}$ is about 5% of its value, due only to the fact that the gradient is not always ideal (as in Fig. 1) nor measured exactly (e.g. choices of what intervals to use in obtaining the needed averages, etc. require judgement). We will also consider the typical uncertainty on |CA| to be 60%, which is large, but the resulting uncertainty on $V_{E,V}$ (for primed or un-primed) is not strongly dependent on |CA|. From Table 1 we see that the average $\Delta(\Delta V_Z)'_{\rm CL}$ is 71 km/s, so for a 5% error we will have a range on this quantity of: (67.5–74.6) km/s. And a range on |CA| is: 0–0.6. Hence, from Eq. (9) we obtain for the MAX value $V'_{E,V}$=46.6 km/s and a MIN value of 33.7 km/s, or V_E is 40±7 km/s. It is evident that for small percent errors in $\Delta(\Delta V_Z)'_{\rm CL}$, as we have here, there will be small errors on $V'_{E,V}$, distinctly smaller than for $V_{E,S}$ in general, which were typically in the range ±(15–20) km/s or larger, if $<V_C>\approx<V_{\rm S-to-E}>$ is a poor assumption for any given case. Let us consider what the error would be for an unusually large $\Delta(\Delta V_Z)'_{\rm CL}$ of say 255 km/s, our largest value (see col. $\Delta V^{\rm m}$ of Table 1), at the same 5% level. This yields 144±23 km/s, i.e. with an error comparable to or slightly larger than those for the scalar V_E's error, but, of course, this is a highly unusual case.

6 Comparisons of V_E to local Alfvén speeds

We now compare the MC expansion speed to various relevant local Alfvén speeds (V_As). In particular, we examine V_A for three points within the ideal MC: the entrance-point (see t=t_{EN} of Fig. 3), the closest approach-point, (at t=t_{CA}), and the exit-point (see t=t_{EX} of Fig. 3). Table 2 shows the Alfvén speeds calculated for these three positions and compares them to the value of $V'_{E,V}$. In almost all cases the V_As are larger than $V'_{E,V}$ (and recall that the $V'_{E,V}$ estimate is usually comparable to the $V_{E,S}$ estimate). There are a few exceptions, however, and for those the V_A is usually close to the value of $V'_{E,V}$. These local Alfvén velocities are on average (for the 53 MCs considered here) equal to $V_{A,EN}$=116 km/s around the inbound boundary, $V_{A,CA}$=137 km/s at closest approach, and $V_{A,EX}$=94 km/s around the outbound boundary; see average values at the bottom of Table 2. Recall that the average values of scalar $V_{E,S}$($<V_{E,S}>$=49 km/s), and vector $V'_{E,V}$ ($<V'_{E,V}>$=44 km/s), are well below these average Alfvén speeds, and, in fact, it is rare that any individual Alfvén speed at these positions is smaller than the associated V_E.

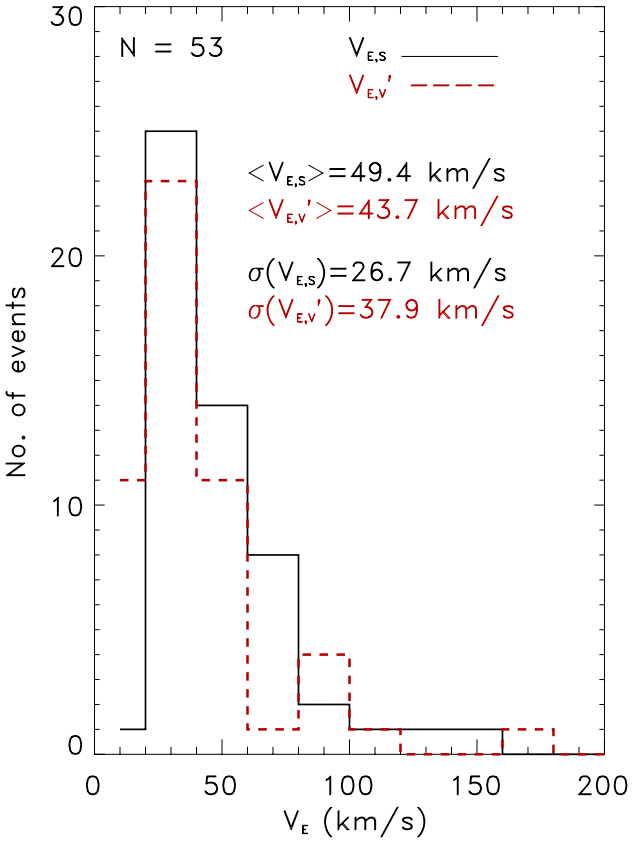

Fig. 7. Histograms of the values derived for $V_{E,S}$ (black) and $V'_{E,V}$ (in red) based on Eqs. (5) and (9), respectively, and where the latter is based on [$|V_{Z,\rm CL}$(MAX)|, $|V_{Z,\rm CL}$(MIN)|], separated by $\Delta t'$]. The peaks for both are at 30 km/s for bucket widths of 20 km/s and the averages and standard deviations (σ) are shown for the two sets. (Note that there is one value of $V'_{E,V}$ of 213 km/s that occurs off-scale and therefore is not shown.)

7 Summary and discussion

Here we have investigated expansion speed of a set (N=53) of well chosen WIND magnetic clouds that occurred over the period from early 1995 to April 2006 by using two separate means of estimation, scalar ($V_{E,S}$) and vector ($V_{E,V}$) methods. Only expansion with respect to the MCs local axis was considered. The "scalar" method uses a well established means of estimation that depends on the average speed of the MC from Sun-to-Earth ($<V_{\rm S-to-E}>$), the local MC's radius (R_O), the duration (T) of spacecraft passage through the MC (at average local speed $<V_C>$), and the assumption that $<V_{\rm S-to-E}>\approx<V_C>$. We actually formulated two vector means of estimating V_E by: (1) using the decrease in $|V_Z|$ (in MC coordinates, where the Z-component is related to spacecraft motion through the MC, as described in Sect. 2) over the full duration (T) and (2) depending only on the decrease in $|V_Z|$ between the $V_{Z,\rm MAX}$ and $V_{Z,\rm MIN}$ values, occurring over $\Delta t'$ (usually a shorter interval than T –

Table 2. Alfvén speeds (V_A) compared to the $V'_{E,V}$ expansion speed.

Start time				$V'_{E,V}$ [a]	B^{b}_{EN}	N_{EN}	$V_{A,EN}$	B^{c}_{C}	N_C	$V_{A,C}$	B^{d}_{EX}	N_{EX}	$V_{A,EX}$
Year	M	D	H	(km/s)	(nT)	(no./cm^{-3})	(km/s)	(nT)	(no./cm^{-3})	(km/s)	(nT)	(no./cm^{-3})	(km/s)
1995	02	08	5.8	27	11	5	111	12	10	85	8	9	60
1995	04	03	7.8	53	8	6	71	10	4	107	7	3	95
1995	08	22	21.3	17	8	16	43	10	10	72	6	19	31
1996	05	27	15.3	31	8	5	76	10	12	63	13	32	49
1996	07	01	17.3	12	7	22	31	14	14	82	9	17	46
1996	08	07	12.3	10	4	11	29	6	10	45	6	9	43
1996	12	24	2.8	54	6	9	42	12	8	92	6	18	31
1997	01	10	5.3	24	14	2	211	14	6	124	20	63	54
1997	06	09	2.3	18	11	16	62	13	17	69	7	11	48
1997	07	15	8.8	14	8	23	38	12	7	104	9	12	59
1997	09	22	0.8	46	14	25	59	17	6	149	10	3	134
1997	10	01	16.3	28	8	9	61	10	7	84	11	3	143
1997	10	10	23.8	36	13	13	79	12	6	101	8	9	60
1997	11	07	15.8	21	14	10	97	17	8	134	14	8	106
1997	11	08	4.9	16	13	5	130	15	4	159	9	9	68
1998	01	07	3.3	24	16	9	114	19	6	166	12	22	57
1998	02	04	4.5	80	7	11	48	13	11	89	6	14	34
1998	03	04	14.3	31	8	17	43	12	12	77	6	27	23
1998	06	02	10.6	7	9	6	78	12	8	95	9	9	62
1998	06	24	16.8	35	9	18	46	13	19	63	16	5	155
1998	08	20	10.3	26	14	5	137	15	5	150	8	6	67
1998	09	25	10.3	89	19	2	283	11	5	113	9	1	187
1998	11	08	23.8	43	20	15	112	14	11	91	10	5	101
1999	08	09	10.8	28	9	5	89	9	8	74	13	11	81
2000	02	21	9.8	45	15	19	73	16	9	117	10	8	78
2000	08	12	6.1	56	25	8	189	24	12	151	15	13	90
2000	10	03	17.1	15	14	7	121	17	13	99	11	6	99
2000	10	13	18.4	11	12	17	65	11	7	94	13	6	117
2000	11	06	23.1	59	15	1	293	22	9	158	21	11	138
2001	03	19	23.3	23	13	14	75	18	5	167	17	18	84
2001	04	04	20.9	98	14	6	129	8	2	133	7	3	95
2001	04	12	7.9	18	20	2	340	14	2	234	7	1	135
2001	04	22	0.9	29	11	9	76	13	10	88	9	13	56
2001	04	29	1.9	43	9	3	107	10	4	118	6	5	64
2001	05	28	11.9	34	9	4	93	9	5	96	8	4	91
2001	07	10	17.3	30	5	5	48	7	4	72	9	6	83
2001	10	31	21.3	35	12	15	71	12	20	56	7	8	53
2001	11	24	15.8	212	10	5	94	15	2	259	10	1	227
2002	03	24	3.8	30	10	12	63	18	2	314	10	16	56
2002	04	18	4.3	31	11	4	119	12	2	208	10	1	205
2002	05	19	3.9	107	21	9	147	11	4	121	7	4	84
2002	08	02	7.4	25	12	12	77	13	5	117	11	6	100
2003	08	18	11.6	58	15	3	178	14	2	209	13	4	154
2003	11	20	10.8	89	24	22	111	37	40	127	12	18	60
2004	04	04	2.8	77	11	2	149	18	11	119	18	7	148
2004	07	24	12.8	50	22	2	394	20	2	291	22	9	153
2004	11	08	3.4	34	44	11	286	17	1	314	7	1	163
2004	11	10	3.6	47	32	11	207	23	7	196	17	5	164
2005	05	15	5.7	173	47	22	220	45	4	524	21	3	287
2005	05	20	7.3	30	11	9	77	17	7	142	7	4	76
2005	06	12	15.6	18	20	16	107	14	2	228	10	8	73
2005	07	17	15.3	25	13	10	85	12	16	67	7	13	43
2006	02	05	19.1	23	10	21	49	10	14	61	6	14	33
Average				44	14	15	116	11	10	137	8	10	94
σ				38	8	6	82	4	6	85	6	10	55

Where:
[a] $V'_{E,V}$ is the vector estimate of expansion velocity based on $|V_{Z,MAX,CL}|$, $|V_{Z,MIN,CL}|$ and $\Delta t'$
[b] EN refers to the entrance point in Fig. 3
[c] C refers to the CA point in Fig. 3
[d] EX refers to the exit point in Fig. 3.

see columns with footnotes a and b in Table 1). The $V_{E,V}$-method also depends on the closest approach distance (Y_O), and the MC's radius (R_O).

The scalar means of estimating V_E is only weakly dependent on any MC parameter fitting model results, but the vector means does depend on quantities that are model dependent (e.g. $|\mathrm{CA}|\equiv|Y_O|/R_O$) and the ability to accurately put **V** into the proper CL system. The most probable values of V_E from both means of estimation are shown to be around 30 km/s, but V_E has larger average values of $<V_{E,S}>$=49 km/s, $<V_{E,V}>$=36 km/s, and $<V'_{E,V}>$=44 km/s, with standard deviations of 27, 38, and 38 km/s, respectively. The correlation between the two sets, $V_{E,S}$ vs. $V'_{E,V}$, gives a c.c. of 0.85. (The linear correlation between $V_{E,S}$ and $V_{E,V}$ is significantly lower, c.c.=0.76.) The average values of V_E are usually below the local Alfvén velocities, which were for the cases examined here equal to 115 km/s around the inbound boundary, 137 km/s at closest approach, and 94 km/s around the outbound boundary. Therefore, a shock upstream of a MC (or any nearby shock) is clearly not expected to be due to MC expansion. Estimates reveal that the errors on the "vector" method of estimating V_E (typically about ±7 km/s, but can get as large as ±25 km/s) are expected to be markedly smaller than those for the scalar method (which is usually in the range ±(15–20) km/s, depending on MC speed). This is true, despite the fact that |CA|, on which the vector method depends, is not always well determined by our MC parameter fitting model (Lepping et al., 1990). This is because the vector method only weakly depends on knowledge of |CA|. It is assumed that $V'_{E,V}$ based on $\Delta(\Delta V_Z)'_{\mathrm{CL}}$, a well determined quantity, probably gives the most faithful estimate of the three means of estimating V_E, and our error analysis confirms this.

In Fig. 8 we show a scatter diagram of $\Delta t'$ vs. T for the full set of 53 MCs, in order to see how well correlated these quantities are, since they alone differentiate the means of obtaining $V_{E,V}$ and $V'_{E,V}$; see Eqs. (8) and (9). As we see, even though $\Delta t'$ is almost always smaller than T (i.e. true in all but six cases), they are fairly well correlated having a c.c. of 0.86. Nevertheless, we see that it is important to distinguish between these two intervals for at least two reasons. First, it tells us that not all of the cross-section of every MC is expanding, which is interesting in itself and suggests a "core" and "annulus" structure with respect to V_E for such MCs, and, second, it provides different estimates of V_E, as we have shown. We then must ask why are the MAX and MIN positions not usually in coincidence with the boundaries? We believe that it is at least partially answered by the fact of the MC's interaction with the surrounding solar wind for most cases. That is to say, we know that most MCs are moving faster than the upstream solar wind causing upstream shock waves in many cases. This accounts for the lack of coincidence at the front of such a MC, since the slower solar wind will cause the plasma in the front-end of the MC to slow down, causing the MAX to occur later within the MC. And sometimes the solar wind behind a MC is moving faster than the rear-end of the MC which will speed up the plasma just within the rear boundary, forcing the MIN point to occur earlier. We do not suggest that these interactions fully explain the lack of agreement of the boundary positions with the MAX and MIN positions, however. Could there also be an association with the MCs' birth conditions? This deserves further study.

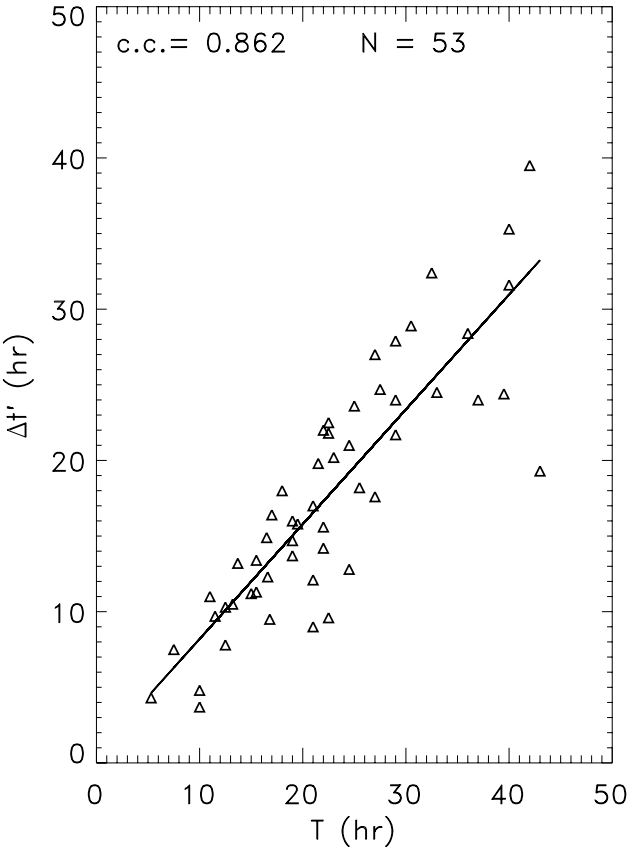

Fig. 8. A scatter diagram of $\Delta t'$ vs. T showing a c.c. of 0.86.

Finally, local Alfvén speeds (V_As) were examined for three points within the ideal MC: the entrance-point (see t=t_{EN} of Fig. 3), the closest approach-point, (at t=t_{CA}), and the exit-point (at t=t_{EX}). This was done to compare these speeds with the expansions speeds, to see if they exceed our V_E-estimates; see Table 2. In essentially all 53 cases studied here the V_As are larger than $V_{E,S}$, $V_{E,V}$, or $V'_{E,V}$. However, there are a few exceptions, but the violations were slight. These local Alfvén velocities are on average equal to $V_{A,EN}$=116 km/s around the inbound MC boundary, $V_{A,CA}$=137 km/s at closest approach, and $V_{A,EX}$=94 km/s at the outbound boundary. As we have seen, the average value of V_E from all methods is around $<V_{E,S}>$=43 km/s, which is well below these average Alfvén speeds. And hardly any individual Alfvén speed at these key positions, for the full

set, is smaller than the associated V_E. Hence, we should not generally expect a shock to be driven by the relatively rapid expansion of any MC at 1 AU. This is consistent with the remarks of Burlaga (1995, Sect. 6.5.1) who studied this effect for earlier cases of MCs at 1 AU. However, upstream shock waves at MCs are observed, of course, and these obviously are due to the larger bulk speed of those MCs compared to their upstream fast mode speeds.

Acknowledgements. We thank the WIND/MFI and SWE teams, and in particular, Keith Ogilvie, the SWE principal investigator, for the care they employ in producing the plasma and field data used in part of this work. We are also grateful to Adam Szabo (GSFC/NASA) and Franco Mariani (Rome) for assistance with the field data. We also thank Tom Narock for assistance in formatting magnetic field data for use in the cloud fitting program. We acknowledge support under the NASA Heliophysics Guest Investigator Program under grant numbers NNX07AH85G and NNG08EF51P.

Topical Editor R. Forsyth thanks M. A. Hidalgo for his help in evaluating this paper.

References

Berdichevsky, D. B., Lepping, R. P., and Farrugia, C. J.: Geometric considerations of the evolution of magnetic flux ropes, Phys. Rev. E, 67, 036405, 2003.

Bothmer, V. and Schwenn, R. H.: Eruptive prominences as sources of magnetic clouds in the solar wind, Space Sci. Rev., 70, 215–220, 1994.

Burlaga, L. F.: Magnetic clouds: Constant alpha force-free configurations, J. Geophys. Res., 93, 7217–7224, 1988.

Burlaga, L. F.: Interplanetary Magnetohydrodynamics, Oxford Univ. Press, New York, 1995.

Burlaga, L. F., Sittler, E., Mariani, F., and Schwenn, R.: Magnetic loop behind an interplanetary shock: Voyager, Helios and IMP-8 observations, J. Geophys. Res., 86, 6673–6684, 1981.

Burlaga, L. F., Lepping, R. P., and Jones, J. A.: Global configuration of a magnetic cloud, Physics of Magnetic Flux Ropes, Geophys. Monogr. Ser., vol. 58, edited by: Russell, C. T., Priest, E. R., and Lee, L. C., p. 373, AGU, Washington, D.C., 1990.

Farrugia, C. J., Burlaga, L. F., Osherovich, V., and Lepping, R. P.: Comparative study of expanding force-free constant alpha magnetic configurations with application to magnetic clouds, in: Solar Wind Seven, edited by: Marsch, E. and Schwenn, T., p 611, Pergamon New York, 1992a.

Farrugia, C. J., Osherovich, V., Burlaga, L. F., Lepping, R. P., and Freeman, M. P.: Radial expansion of an ideal MHD configuration and the temporal development of the magnetic field, in: Solar Wind Seven, edited by: Marsch, E. and Schwenn, T., p 615, Pergamon New York, 1992b.

Farrugia, C. J., Burlaga, L. F., Osherovich, V., Richardson, I. G., Freeman, M. P., Lepping, R. P., and Lazarus, A. J.: A study of an expanding interplanetary magnetic cloud and its interaction with the earth's magnetosphere, The interplanetary aspect, J. Geophys. Res., 98, 7621–7632, 1993.

Goldstein, H.: On the field configuration in magnetic clouds, in: Solar Wind Five, edited by: Neugebauer, M., NASA Conf. Publ., 2280, 731–733, 1983.

Gopalswamy, N., Hanaoka, Y., Kosugi, T., Lepping, R. P., Steinberg, J. T., Plunkett, S., Howard, R. A., Thompson, B. J., Gurman, J., Ho, G., Nitta, N., and Hudson, H. S.: On the relationship between coronal mass ejections and magnetic clouds, Geophys. Res. Lett., 25, 2485–2488, 1998.

Gopalswamy, A., Lara, R., Lepping, P., Kaiser, M. L., Berdichevsky, D., and St. Cyr, O. C.: Interplanetary acceleration of coronal mass ejections, Geophys. Res. Lett., 27, 145–148, 2000.

Gosling, J. T.: Coronal mass ejections and magnetic flux ropes in interplanetary space, Physics of Magnetic Flux Ropes, Geophys. Monogr. Ser., vol. 58, edited by: Russell, C. T., Priest, E. R., and Lee, L. C., p. 343, AGU, Washington, D.C., 1990.

Gosling, J. T.: Coronal mass ejections: An overview, in: Coronal Mass Ejections, edited by: Crooker, N., Joselyn, J. A., Feynmann, J., et al., GM 99, p. 9, Washington, D.C., American Geophysical Union, 1997.

Hidalgo, M. A.: A study of the expansion and distortion of the cross section of magnetic clouds in the interplanetary medium, J. Geophys. Res., 108(A8), 1320, doi:10.1029/2002JA009818, 2003.

Hidalgo, M. A.: Correction to "A study of the expansion and distortion of the cross section of magnetic clouds in the interplanetary medium," J. Geophys. Res., 110, A03207, doi:10.1029/2004JA010752, 2005.

Hidalgo, M. A., Cid, C., Vinas, A. F., and Sequeiros, J.: A non-force free approach to the topology of magnetic clouds in the solar wind, J. Geophys. Res., 107, A1, doi:10.1029/2001JA900100, 2002.

Lepping, R. P., Jones, J. A., and Burlaga, L. F.: Magnetic field structure of interplanetary magnetic clouds at 1 AU, J. Geophys. Res., 95, 11 957–11 965, 1990.

Lepping, R. P., Acuña, M. H., Bulaga, L. F., et al.: The WIND magnetic field investigation, The Global Geospace Mission, Space Sci. Rev., 71, 207–229, 1995.

Lepping, R. P., Berdichevsky, D., Szabo, A., Goodman, M., and Jones, J.: Modification of magnetic cloud model: Elliptical cross-section, AGU EOS Transactions (SH11A-05), 79, F696, 1998.

Lepping, R. P., Berdichevsky, D., Szabo, A., Lazarus, A. J., and Thompson, B. J.: Upstream shocks and interplanetary magnetic cloud speed and expansion: Sun, WIND, and Earth observations, Space Weather Study using Multipoint Techniques, Pergamon, Elsevier Science, New York, 87, 2002.

Lepping, R. P., Berdichevsky, D., and Ferguson, T.: Estimated Errors in Magnetic Cloud Model Fit-Parameters with Force Free Cylindrically Symmetric Assumptions, J. Geophys. Res., 108(A10), 1356, doi:10.1029/2002JA009657, 2003a.

Lepping, R. P., Berdichevsky, D., Szabo, A., Arqueros, C., and Lazarus, A. J.: Profile of an Average Magnetic Cloud at 1 AU for the Quiet Solar Phase: WIND Observations, Solar Phys., 212, 425–444, 2003b.

Lepping, R. P., Berdichevsky, D. B., Wu, C.-C., Szabo, A., Narock, T., Mariani, F., Lazarus, A. J., and Quivers, A. J.: A Summary of WIND Magnetic Clouds for the Years 1995–2003: Model-Fitted Parameters, Associated Errors, and Classifications, Ann. Geophys., 24, 215–245, 2006, http://www.ann-geophys.net/24/215/2006/.

Lepping, R. P. and Wu, C.-C.: On the variation of interplanetary magnetic cloud type through solar cycle 23: WIND events, J.

Geophys. Res., 112, A10103, doi:10.1029/2006JA012140, 2007.
Marubashi, K.: Structure of the interplanetary magnetic clouds and their solar origins, Adv. Space Res., 6(6), 335–338, 1986.
Marubashi, K.: Interplanetary magnetic flux ropes and solar filaments, in: Coronal Mass Ejections, edited by: Crooker, N., Joselyn, J. A., Feynmann, J., et al., GM 99, p. 147, Washington, D.C., American Geophysical Union, 1997.
Mulligan, T. and Russell, C. T.: Multispacecraft modeling of the flux rope structure of interplanetary coronal mass ejections: Cylindrically symmetric versus non-symmetric topologies, J. Geophys. Res., 106(A6), 10 581–10 596, 2001.
Nieves-Chinchilla, T., Hidalgo, M. A., and Sequeiros, J.: Magnetic clouds observed at 1 AU during the period 2000–2003, Solar Phys., 232, 105–126, 2005.
Ogilvie, K. W., Chomay, D. J., Fritzenreiter, R. J., et al.: SWE, A comprehensive plasma instrument for the WIND spacecraft, The Global Geospace Mission, Space Sci. Rev., 71, 55–99, 1995.
Osherovich, V. I., Farrugia, C. J., and Burlaga, L. F.: Dynamics of aging magnetic clouds, Adv. Space Res., 13(6), 57–62, 1993.
Osherovich, V. A., Farrugia, C. J., and Burlaga, L. F.: The nonlinear evolution of magnetic flux ropes, 2, Finite beta plasma, J. Geophys. Res., 100, 12 307–12 318, 1995.
Riley, P. and Crooker, N. U.: Kinematic treatment of coronal mass ejection evolution in the solar wind, Ap. J., 600, 1035–1042, 2004.
Riley, P., Linker, J. A., Lionello, R., Mikic, Z., Odstrcil, D., Hidalgo, M. A., Cid, C, Hu, Q., Lepping, R. P., Lynch, B. J., and Rees, A.: Fitting flux ropes to a global MHD solution: A comparison of techniques, J. Atmos. Sol.-Terr. Phys., 66(15–16), 1321–1331, 2004.
Vandas, M., Odstrcil, D., and Watari, S.: Three-dimensional MHD simulation of a loop-like magnetic cloud in the solar wind, J. Geophys. Res., 107(A9), 1236, doi:10.1029/2001JA005068, 2002.
Vandas, M. and Romashets, E. P.: Force-free field with constant alpha in an oblate cylinder: A generalization of the Lundquist solution, Astron. Astrophys., 398, 801–807, 2003.
Vandas, M., Romashets, E. P., Watari, S., Geranios, A., Antoniadou, E., and Zacharopoulou, O.: Comparison of force-free flux rope models with observations of magnetic clouds, Adv. Space Res., 38, 441–445, 2006.